Contribution from the Laboratoire de Chimie de Coordination du CNRS, Unité No. 8241 liée par convention à l'Université Paul Sabatier, 205 route de Narbonne, 31077 Toulouse Cedex, France

Synthesis, Structure, and Magnetic Properties of a Dodecamanganese(II) Complex Afforded by a Binucleating Acyclic N_2O_3 Schiff Base

Dominique Luneau, Jean-Michel Savariault, and Jean-Pierre Tuchagues*

Received April 14, 1988

The synthesis, IR and EPR spectra, and variable-temperature magnetic susceptibility of the novel dodecanuclear manganese(II) complex $[(Mn_2C_{21}H_{15}N_2O_3)_6(OH)_4(CH_3CO_2)_2]$ are described. $C_{21}H_{15}N_2O_3$ (L) is the fully deprotonated form of the binucleating acyclic LH_3 ligand including an N_2O_3 donor set and resulting from the condensation of 2,6-diformyl-4-methylphenol with 2-aminophenol. The crystal molecular structure of $[(Mn_2L)_6(OH)_4(CH_3CO_2)_2]\cdot 2Et_2O\cdot H_2O$ has been established by X-ray diffraction methods. This complex crystallizes in the monoclinic system, space group $P2_1/n$, in a cell of dimensions a = 26.605 (8) Å, b = 17.237 (5) Å, c = 31.250 (8) Å, and β = 112.11 (3)° with Z = 4. The structure was solved by direct methods and refined by a succession of difference Fourier syntheses and least-squares refinements. Due to the large number of variables and limited number of reflections, a block refinement of the Mn_2L subunits was carried out, leading to agreement indices R = 0.070 and R_w = 0.091 with 6190 unique reflections for which $F_o^2 > 3\sigma(F_o^2)$. The results obtained provide evidence that each dodecanuclear asymmetric aggregate is built from six binuclear units whose space arrangement corresponds to a 10 Å radius sphere. The twelve manganese(II) ions constitute two crowns of six metal ions held together by twenty-two oxygen atoms pertaining either to the six L ligands or to the four hydroxo moieties. Each crown is capped by a bridging acetate anion in either a bis-bidentate or a bidentate coordination mode. Each of the twelve manganese(II) ions is oxygen-bridged to four nearest manganese neighbors with Mn···Mn distances ranging from 3.16 to 4.14 Å. This structural arrangement affords a large predominance of the antiferromagnetic interactions in the aggregate ($J_{av} \sim -3$ cm^{-1}). The EPR spectra of this dodecanuclear manganese(II) aggregate afford the first example of inhomogeneous exchange narrowing in frozen solution.

Introduction

As part of our involvement in the study of the structural and magnetic properties of manganese complexes with polydentate ligands,[1] we have prepared and studied a new manganese(II) complex based on the binucleating acyclic ligand LH_3 including an N_2O_3 donor set. LH_3 has been initially described by Robson[2] and is schematized in Figure 1a. By reacting LH_3 with copper(II) salts, Robson[2,3] was able to prepare and characterize several binuclear copper(II) complexes of general formula Cu^{II}_2LX (X = OR^-, OH^-, $C_3H_3N_2^-$) (Figure 1b).

Later, Hoskins et al.[4] described several cobalt and nickel complexes resulting from the reaction of LH_3 with cobalt(II) and nickel(II) salts under a variety of conditions. On the basis of X-ray single crystal diffraction studies, one of these complexes was identified as a tetranuclear compound including two $Co^{II}L(CH_3CO_2)Co^{III}$ moieties bridged by two μ_3-hydroxo oxygen atoms (Figure 1c). In each binuclear unit, the Co(II) and Co(III) ions are bridged through the central phenolate oxygen of L, the acetato group, and one hydroxo group. From molecular weight and conductivity measurements, the nickel(II) complexes were assumed to involve similar neutral tetranuclear species.

Upon reacting LH_3 with a manganese(II) salt, our goal was to prepare a tetranuclear manganese compound. This paper describes the synthesis and characterization (elemental analyses, IR spectroscopy, and X-ray single-crystal molecular structure) of the unexpected dodecanuclear $[(Mn^{II}_2L)_6(OH)_4(CH_3CO_2)_2]$ complex resulting from this reaction. The magnetic properties of this new dodecanuclear manganese(II) species have been investigated with EPR and variable-temperature magnetic susceptibility measurements.

Experimental Section

Materials. 2-Aminophenol (Aldrich) was sublimed prior to use. 2,6-Diformyl-4-methylphenol was prepared according to literature methods.[5,6] All other chemicals were of reagent grade or equivalent purity.

Table I. Crystallographic Data for $[(Mn_2L)_6(OH)_4(CH_3CO_2)_2]$

formula: $C_{138}H_{122}N_{12}O_{29}Mn_{12}$	fw 3071.8
a = 26.605 (8) Å	space group: $P2_1/n$ (No. 14)
b = 17.237 (5) Å	T = 20 °C
c = 31.250 (8) Å	λ = 0.7107 Å
β = 112.11 (3)°	ρ_{obsd} = 1.50 (3) g cm^{-3}, ρ_{calcd} = 1.53 g cm^{-3}
V = 13277.1 Å^3	μ(Mo Kα) = 11.26 cm^{-1}
Z = 4	$R(F_o)$ = 0.070
	$R_w(F_o)$ = 0.091

Ligand. LH_3 was prepared according to the procedure reported by Robson.[2] The elemental analyses and IR spectroscopy are in agreement with the previously reported data.

Complex. $[(Mn_2L)_6(OH)_4(CH_3CO_2)_2]$ was prepared by addition of a deoxygenated methanolic solution of manganese(II) acetate tetrahydrate to a deoxygenated methanolic suspension of the LH_3 ligand (2:1 ratio). The resulting reaction mixture was warmed to 65 °C for 2 h. The orange-red microcrystalline product was filtered off, washed twice with methanol, and dried under vacuum for 6 h. The manganese(II) complex was also prepared through an in situ reaction by addition of the manganese salt solution to the ligand reaction mixture.

As an added precaution, all complex preparations were carried out in Schlenk glassware under purified nitrogen atmosphere. The complex samples were directly transferred and stored in an inert-atmosphere box (Vacuum Atmosphere H.E.43-2) equipped with a dry train (Jahan EVAC 7).

The analytical results (Calcd: C, 52.00; H, 4.45; N, 5.06; Mn, 19.86. Found: C, 51.69; H, 4.57; N, 4.45; Mn, 19.37) are consistent with the presence of methanol in the 1:1 Mn:MeOH ratio.

Physical Measurements. Elemental analyses were carried out at the microanalytical laboratory of the Laboratoire de Chimie de Coordination, Toulouse, France, for C, H, and N and at the Service Central de Microanalyse du CNRS, Vernaison, France, for Mn.

IR spectra were recorded on a Perkin-Elmer 983 spectrophotometer coupled with a Perkin-Elmer infrared data station. Samples were run as CsBr pellets prepared under nitrogen in the drybox.

Variable-temperature magnetic susceptibility data were obtained as previously described[7] on polycrystalline samples with a Faraday-type magnetometer equipped with a continuous-flow Oxford Instruments cryostat.

Least-squares computer fittings of the magnetic susceptibility data were carried out with an adapted version of the function-minimization program, STEPT.[8]

(1) Mabad, B.; Cassoux, P.; Tuchagues, J.-P.; Hendrickson, D. N. *Inorg. Chem.* **1986**, *25*, 1420-1431.
(2) Robson, R. *Aust. J. Chem.* **1970**, *23*, 2217-2224.
(3) Robson, R. *J. Inorg. Nucl. Chem.* **1970**, *6*, 125-128.
(4) Hoskins, B. F.; Robson, R.; Vince, D. *J. Chem. Soc., Chem. Commun.* **1973**, 392-393.
(5) Gagné, R. R.; Spiro, C. L.; Smith, T. J.; Haman, C. A.; Thies, W. R.; Shiemke, A. K. *J. Am. Chem. Soc.* **1981**, *103*, 4073.
(6) Ullman, F.; Brittner, K. *Chem. Ber.* **1909**, *42*, 2539.
(7) Luneau, D.; Savariault, J.-M.; Cassoux, P.; Tuchagues, J.-P. *J. Chem. Soc., Dalton Trans.* **1988**, 1225-1235.
(8) Chandler, J. P. Quantum Chemistry Program Exchange, Indiana University, Program 66.

0020-1669/88/1327-3912$01.50/0 © 1988 American Chemical Society

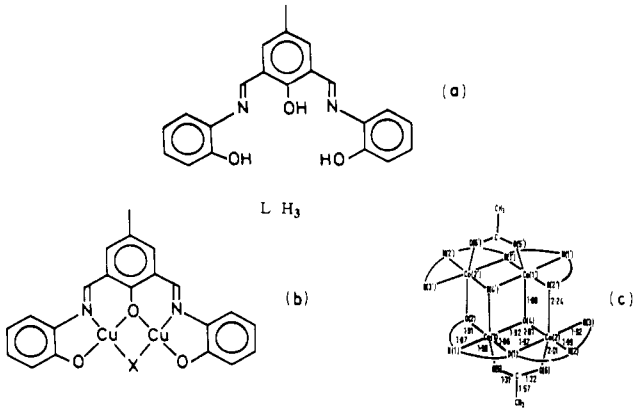

Figure 1. Schematic representation of (a) the LH_3 ligand, (b) the copper dimers, and (c) the cobalt tetramers obtained from LH_3.

EPR spectra were obtained on a Bruker 200 TT spectrometer equipped as previously described.[1]

Structure Determination of $[(Mn_2L)_6(OH)_4(CH_3CO_2)_2]\cdot 2Et_2O\cdot H_2O$. Opaque red parallelepiped crystals were obtained by slow concentration of a diethyl ether solution of the manganese(II) complex in the drybox. These crystals belong to the monoclinic system, space group $P2_1/n$. The selected crystal was a parallelepiped of approximate dimensions 0.25 × 0.15 × 0.15 mm. It was sealed on a glass fiber and mounted on an Enraf-Nonius CAD4 diffractometer. Cell constants were obtained from a least-squares fit of the setting angles of 25 reflections. Crystal and intensity collection data are summarized in Table I. A total of 14 184 reflections were recorded at 20 °C in the 2–42° 2θ (Mo Kα) range by procedures described elsewhere.[9] Intensity standards, recorded periodically, showed no significant variations during measurements. Reflections were corrected for Lorentz and polarization effects,[10] 6190 of which with $I > 3\sigma(I)$ were used in subsequent calculations. No absorption corrections were made ($\mu r \sim 0.02$).

Structure Solution and Refinement. The starting point of the structure was determined by using direct methods.[11] A succession of difference Fourier syntheses and least-squares refinements revealed the positions of 180 non-hydrogen atoms belonging to the complex entity. Residues in the Fourier difference were attributed to one water and two diethyl ether solvent molecules, a disorder of one C_2H_5 part of both ether molecules being observed.

Due to the large number of variables, the carbon atoms of the phenyl groups and all non-hydrogen atoms of the solvent molecules were refined isotropically. All other non-hydrogen atoms were refined anisotropically. The hydrogen atoms of the phenyl groups were introduced at 0.95 Å from the carbon atoms and their thermal parameters set isotropically to U_{iso} = 0.065 Å^2; they were not refined.

The full-matrix refinement of such a large asymmetric entity involves a very large number of variables, thus requiring a lengthy and expensive computation. To offset this problem, a block-matrix refinement was performed by using a seven-cycle combination including six Mn_2L blocks and one acetate and solvent molecules block.

A careful examination of the observed and calculated structure factors vs sin θ revealed extinction phenomena. An empirical correction, $F = F(1 - gF^2/\sin\theta)$ was consequently applied.[11]

The atomic scattering factors used were those proposed by Cromer and Waber[12] with anomalous dispersion effects.[13] The final block-matrix least-squares refinement, minimizing $\sum w(|F_o| - |F_c|)^2$, converged to $R = \sum||F_o| - |F_c||/\sum|F_o| = 0.070$ and $R_w = [\sum w(|F_o| - |F_c|)^2/\sum w|F_o|^2]^{1/2} = 0.091$. The goodness of fit was $S = 3.4$ with 6190 observations and 1134 variables.

All calculations were performed on a VAX 11/730 DEC computer using the programs SHELX-86,[11] SHELX-76,[14] and ORTEP[15] and several local subroutines written by J. Aussoleil, F. Dahan, and J.-M. Savariault.

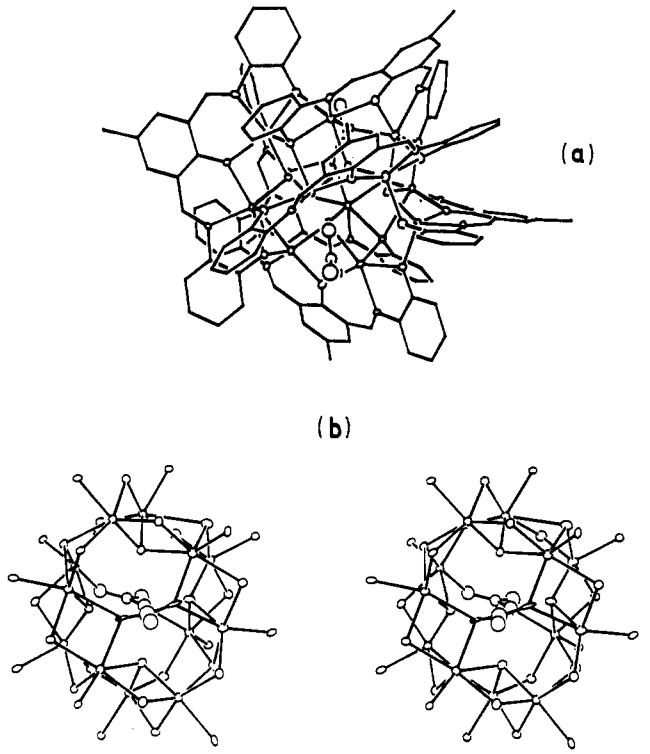

Figure 2. (a) ORTEP view of the asymmetric dodecanuclear aggregate $[(Mn_2L)_6(OH)_4(CH_3CO_2)_2]$. (b) Stereoview of the manganese, oxygen, and nitrogen atoms of its core.

The asymmetric dodecanuclear unit of $[(Mn_2L)_6(OH)_4(CH_3CO_2)_2]$ and the manganese, oxygen, and nitrogen atoms of its core are shown in Figure 2. Final fractional atomic coordinates with their estimated standard deviations are given in Table II.

Results and Discussion

Infrared Spectroscopy. The infrared spectrum exhibits a strong and broad absorption at 1583 cm^{-1}. This observation is in agreement with the description of the IR spectrum of $Cu_2L(CH_3O)$ given by Robson.[2] The strong 1583-cm^{-1} absorption is attributed to the stretching mode of the C=N functions. However, this absorption is broader in the case of the manganese complex, which can be attributed to the superimposition of the asymmetric stretching mode of the carboxylate functions, the presence of which has been confirmed by the molecular structure determination. The absorption observed at 1440 cm^{-1} for the manganese complex is characteristic of the symmetric stretching mode of the acetato group. No similar absorption has been observed for the copper complex[2] in which no carboxylic function has been identified. The $\Delta\nu$ separation between the symmetric and asymmetric C–O stretches is typical of bidentate bridging acetato groups.[16-19]

Molecular Structure of $[(Mn_2L)_6(OH)_4(CH_3CO_2)_2]$. The unit cell includes four asymmetric dodecanuclear units.[20]

Each dodecanuclear asymmetric aggregate is built for six binuclear units (A, B, C, D, E, and F), whose basic structure is imposed by the L ligand (Figure 3). For the sake of clarity, we have used the same numbering for the atoms pertaining to all six binuclear units and indicated their belonging to one of the six binuclear units with the a (unit A), b (unit B), ... subscripts. The full labeling scheme for the binuclear units is given in Figure 4.

(9) Mosset, A.; Bonnet, J.-J.; Galy, J. *Acta Crystallogr., Sect. B: Struct. Crystallogr. Cryst. Chem.* **1977**, *B33*, 2639–2644.
(10) Frentz, B. A. *SDP-Structure Determination Package*; Enraf-Nonius: Delft, 1982.
(11) Sheldrick, G. M. In *Crystallographic Computing 3*; Sheldrick, G. M., Krüger, C., Goddard, R., Eds.; Oxford University Press: Oxford, U.K., 1985; pp 175–179.
(12) Cromer, D. T.; Waber, J. T. In *International Tables for X-ray Crystallography*; Kynoch: Birmingham, U.K., 1974; Vol. IV, Table 2.2.B, pp 99,101.
(13) Cromer, D. T. Reference 12, Table 2.3.1, p 149.
(14) Sheldrick, G. M. "SHELX 76. Program for Crystal Structure Determination"; University of Cambridge: Cambridge, U.K., 1976.
(15) Johnson, C. K. "ORTEP"; Report ORNL-1794; Oak Ridge National Laboratory: Oak Ridge, TN, 1965.
(16) Torihara, N.; Mikuriya, M.; Okawa, H.; Kida, S. *Bull. Chem. Soc. Jpn.* **1980**, 392–393.
(17) Deacon, G. B.; Phillips, R. J. *Coord. Chem. Rev.* **1980**, *33*, 227–250.
(18) Wieghardt, K.; Bossek, U.; Ventur, D.; Weiss, J. *J. Chem. Soc., Chem. Commun.* **1985**, 347–349.
(19) Nakamoto, K. *Infrared and Raman Spectra of Inorganic and Coordination Compounds*, 4th ed.; Wiley: New York, 1986; p 231.
(20) Supplementary material.

Table II. Positional Parameters and Their Estimated Standard Deviations[a]

atom	x/a	y/b	z/c	B, Å²	atom	x/a	y/b	z/c	B, Å²
Mn(1a)	0.3611 (1)	0.7043 (1)	0.13869 (9)	4.06 (9)	C(13c)	0.7421 (6)	0.8320 (9)	0.2268 (6)	3.5 (4)*
Mn(2a)	0.4713 (1)	0.6164 (1)	0.15372 (9)	3.87 (8)	C(14c)	0.6938 (7)	0.8030 (9)	0.1909 (6)	3.9 (4)*
O(1a)	0.3109 (4)	0.7716 (6)	0.1657 (3)	4.3 (4)	C(15c)	0.7537 (6)	0.8344 (9)	0.2745 (6)	3.7 (6)
O(2a)	0.3863 (4)	0.6073 (6)	0.1090 (3)	3.8 (3)	C(16c)	0.7385 (7)	0.8133 (9)	0.3433 (6)	3.9 (4)*
O(3a)	0.5569 (4)	0.6187 (6)	0.1741 (3)	3.9 (4)	C(17c)	0.7912 (8)	0.788 (1)	0.3723 (7)	5.6 (5)*
O(4a)	0.4454 (4)	0.7248 (6)	0.1689 (4)	4.3 (4)	C(18c)	0.8046 (8)	0.784 (1)	0.4183 (7)	6.2 (5)*
N(1a)	0.2812 (5)	0.6513 (8)	0.1074 (5)	4.0 (5)	C(19c)	0.7676 (9)	0.801 (1)	0.4373 (7)	7.3 (5)*
N(2a)	0.4815 (6)	0.5452 (7)	0.0993 (5)	3.9 (5)	C(20c)	0.7154 (8)	0.819 (1)	0.4092 (7)	5.8 (5)*
C(1a)	0.2608 (8)	0.744 (1)	0.1526 (6)	3.9 (4)*	Mn(1d)	0.5425 (1)	1.0113 (1)	0.27095 (8)	3.99 (8)
C(2a)	0.2221 (8)	0.780 (1)	0.1678 (6)	5.2 (5)*	Mn(2d)	0.5814 (1)	0.8786 (1)	0.34695 (8)	4.03 (8)
C(3a)	0.1731 (8)	0.755 (1)	0.1559 (6)	5.3 (4)*	O(1d)	0.5246 (4)	1.0410 (5)	0.2010 (3)	3.8 (3)
C(4a)	0.1559 (8)	0.691 (1)	0.1288 (6)	6.1 (5)*	O(2d)	0.5888 (4)	1.0005 (5)	0.3435 (3)	4.2 (3)
C(5a)	0.1900 (8)	0.656 (1)	0.1119 (6)	5.5 (4)*	O(3d)	0.5597 (4)	0.7732 (6)	0.3688 (4)	5.3 (4)
C(6a)	0.2434 (8)	0.683 (1)	0.1232 (6)	4.0 (4)*	O(4d)	0.5232 (4)	0.8951 (5)	0.2807 (3)	4.3 (3)
C(7a)	0.2671 (7)	0.609 (1)	0.0693 (6)	4.0 (6)	N(1d)	0.5875 (5)	1.1180 (7)	0.2772 (5)	3.4 (4)
C(8a)	0.3022 (7)	0.5728 (9)	0.0512 (6)	3.9 (4)*	N(2d)	0.5988 (5)	0.9018 (9)	0.4202 (4)	4.2 (5)
C(9a)	0.2767 (8)	0.537 (1)	0.0067 (7)	6.3 (5)*	C(1d)	0.5483 (6)	1.1043 (9)	0.1954 (5)	3.1 (3)*
C(10a)	0.3020 (9)	0.498 (1)	−0.0169 (7)	6.7 (5)*	C(2d)	0.5401 (7)	1.131 (1)	0.1503 (6)	5.2 (4)*
C(11a)	0.2714 (8)	0.463 (1)	−0.0656 (6)	10.7 (8)	C(3d)	0.5686 (8)	1.196 (1)	0.1452 (6)	6.3 (5)*
C(12a)	0.3586 (8)	0.499 (1)	0.0040 (6)	5.6 (5)*	C(4d)	0.6014 (8)	1.235 (1)	0.1820 (7)	6.1 (5)*
C(13a)	0.3881 (7)	0.5339 (9)	0.0463 (6)	3.8 (4)*	C(5d)	0.6123 (7)	1.2117 (9)	0.2267 (6)	5.0 (4)*
C(14a)	0.3614 (7)	0.5720 (9)	0.0710 (6)	3.8 (4)*	C(6d)	0.5826 (7)	1.1480 (9)	0.2333 (6)	4.0 (4)*
C(15a)	0.4462 (7)	0.525 (1)	0.0605 (6)	4.1 (6)	C(7d)	0.6151 (7)	1.1522 (9)	0.3161 (7)	4.5 (6)
C(16a)	0.5376 (8)	0.527 (1)	0.1128 (7)	4.7 (5)*	C(8d)	0.6220 (7)	1.127 (1)	0.3613 (7)	5.1 (4)*
C(17a)	0.5580 (8)	0.476 (1)	0.0876 (6)	6.2 (5)*	C(9d)	0.6437 (8)	1.186 (1)	0.3968 (7)	7.0 (5)*
C(18a)	0.6145 (9)	0.458 (1)	0.1033 (7)	6.7 (5)*	C(10d)	0.6539 (9)	1.172 (1)	0.4439 (8)	8.8 (6)*
C(19a)	0.6482 (8)	0.493 (1)	0.1438 (7)	6.1 (5)*	C(11d)	0.678 (1)	1.239 (1)	0.4814 (7)	15 (1)
C(20a)	0.6289 (7)	0.5455 (9)	0.1668 (6)	4.0 (4)*	C(12d)	0.6406 (8)	1.097 (1)	0.4548 (6)	7.2 (5)*
C(21a)	0.5739 (7)	0.568 (1)	0.1504 (6)	4.2 (4)*	C(13d)	0.6188 (6)	1.039 (1)	0.4209 (6)	4.3 (4)*
Mn(1b)	0.4492 (1)	0.8192 (2)	0.11331 (9)	4.14 (8)	C(14d)	0.6088 (6)	1.053 (1)	0.3744 (6)	3.9 (4)*
Mn(2b)	0.5440 (1)	0.9330 (2)	0.17932 (9)	4.36 (9)	C(15d)	0.6110 (6)	0.967 (1)	0.4399 (6)	4.3 (6)
O(1b)	0.3663 (4)	0.7894 (6)	0.0925 (4)	4.8 (4)	C(16d)	0.5948 (7)	0.832 (1)	0.4419 (6)	4.9 (4)*
O(2b)	0.5112 (4)	0.9062 (6)	0.1093 (3)	4.3 (4)	C(17d)	0.6071 (8)	0.825 (1)	0.4912 (7)	6.9 (5)*
O(3b)	0.6131 (4)	0.9396 (6)	0.2473 (3)	3.9 (3)	C(18d)	0.6004 (9)	0.752 (1)	0.5073 (8)	9.1 (6)*
N(1b)	0.4093 (5)	0.8677 (7)	0.0423 (4)	3.6 (4)	C(19d)	0.5835 (9)	0.689 (1)	0.4816 (8)	8.2 (6)*
N(2b)	0.6132 (5)	0.9704 (7)	0.1627 (5)	4.2 (5)	C(20d)	0.5710 (7)	0.695 (1)	0.4348 (7)	6.1 (5)*
C(1b)	0.3326 (7)	0.8235 (9)	0.0550 (6)	4.1 (4)*	C(21d)	0.5756 (7)	0.767 (1)	0.4148 (7)	5.0 (4)*
C(2b)	0.2754 (7)	0.820 (1)	0.0428 (6)	5.7 (4)*	Mn(1e)	0.4759 (1)	0.7670 (2)	0.33932 (9)	5.6 (1)
C(3b)	0.2422 (8)	0.860 (1)	0.0029 (7)	7.7 (5)*	Mn(2e)	0.4626 (1)	0.6331 (1)	0.26510 (9)	4.50 (9)
C(4b)	0.2622 (9)	0.895 (1)	−0.0247 (7)	7.0 (5)*	O(1e)	0.4724 (4)	0.8881 (6)	0.3461 (3)	4.7 (4)
C(5b)	0.3178 (8)	0.898 (1)	−0.0132 (6)	5.9 (5)*	O(2e)	0.4528 (4)	0.6524 (6)	0.3338 (4)	4.7 (4)
C(6b)	0.3517 (7)	0.8628 (9)	0.0266 (6)	4.0 (4)*	O(3e)	0.4682 (4)	0.5579 (6)	0.2108 (4)	5.0 (4)
C(7b)	0.4333 (7)	0.8829 (9)	0.0156 (6)	3.9 (6)	O(4e)	0.4489 (4)	0.7638 (6)	0.2697 (3)	5.1 (4)
C(8b)	0.4918 (7)	0.8973 (9)	0.0285 (6)	4.3 (4)*	N(1e)	0.4401 (5)	0.7763 (8)	0.3900 (4)	4.0 (5)
C(9b)	0.5113 (7)	0.8988 (9)	−0.0067 (6)	4.7 (4)*	N(2e)	0.4678 (5)	0.5138 (8)	0.2931 (4)	4.1 (5)
C(10b)	0.5658 (8)	0.916 (1)	−0.0001 (6)	5.3 (4)*	C(1e)	0.4609 (6)	0.9103 (9)	0.3829 (6)	4.4 (4)*
C(11b)	0.5857 (8)	0.917 (1)	−0.410 (6)	7.1 (8)	C(2e)	0.4652 (7)	0.988 (1)	0.3978 (6)	5.0 (4)*
C(12b)	0.5983 (7)	0.9359 (9)	0.0451 (6)	4.5 (4)*	C(3e)	0.4520 (8)	1.006 (1)	0.4354 (7)	6.3 (5)*
C(13b)	0.5822 (7)	0.9356 (9)	0.0830 (6)	4.1 (4)*	C(4e)	0.4397 (8)	0.953 (1)	0.4602 (7)	7.8 (5)*
C(14b)	0.5286 (6)	0.9132 (8)	0.0759 (6)	3.4 (4)*	C(5e)	0.4349 (8)	0.876 (1)	0.4471 (7)	6.7 (5)*
C(15b)	0.6212 (7)	0.9615 (9)	0.1253 (6)	4.2 (6)	C(6e)	0.4442 (7)	0.854 (1)	0.4078 (6)	5.1 (4)*
C(16b)	0.6552 (6)	1.0044 (8)	0.2039 (5)	3.1 (3)*	C(7e)	0.4143 (7)	0.724 (1)	0.4034 (6)	5.0 (6)
C(17b)	0.6926 (7)	1.061 (1)	0.2001 (6)	5.1 (4)*	C(8e)	0.4090 (6)	0.643 (1)	0.3888 (5)	4.4 (4)*
C(18b)	0.7303 (8)	1.092 (1)	0.2406 (7)	6.0 (5)*	C(9e)	0.3805 (7)	0.598 (1)	0.4092 (6)	5.1 (4)*
C(19b)	0.7274 (7)	1.073 (1)	0.2815 (6)	5.2 (4)*	C(10e)	0.3733 (7)	0.517 (1)	0.3997 (6)	5.7 (4)*
C(20b)	0.6907 (7)	1.0210 (9)	0.2861 (5)	4.0 (4)*	C(11e)	0.340 (1)	0.468 (1)	0.4228 (7)	8.6 (9)
C(21b)	0.6531 (7)	0.9842 (9)	0.2463 (6)	3.8 (4)*	C(12e)	0.3965 (7)	0.4860 (9)	0.3718 (6)	4.9 (4)*
Mn(1c)	0.5771 (1)	0.7312 (2)	0.16555 (9)	4.52 (9)	C(13e)	0.4243 (7)	0.529 (1)	0.3493 (6)	4.6 (4)*
Mn(2c)	0.6317 (1)	0.8191 (1)	0.26232 (8)	4.06 (8)	C(14e)	0.4301 (6)	0.612 (1)	0.3565 (5)	3.9 (4)*
O(1c)	0.4994 (4)	0.7309 (6)	0.1048 (4)	4.3 (4)	C(15e)	0.4450 (7)	0.490 (1)	0.3199 (7)	5.4 (7)
O(2c)	0.6544 (4)	0.7802 (6)	0.2035 (4)	4.8 (4)	C(16e)	0.4876 (6)	0.4631 (9)	0.2681 (6)	3.6 (4)*
O(3c)	0.6493 (4)	0.8436 (6)	0.3346 (4)	4.8 (4)	C(17e)	0.5093 (7)	0.389 (1)	0.2865 (6)	5.5 (4)*
O(4c)	0.5510 (4)	0.8139 (6)	0.2002 (4)	5.2 (4)	C(18e)	0.5287 (7)	0.342 (1)	0.2593 (7)	6.1 (5)*
N(1c)	0.6027 (6)	0.7399 (8)	0.1078 (4)	4.2 (5)	C(19e)	0.5235 (8)	0.361 (1)	0.2167 (7)	8.0 (6)*
N(2c)	0.7209 (5)	0.8170 (7)	0.2948 (4)	3.4 (4)	C(20e)	0.5031 (7)	0.435 (1)	0.1987 (6)	5.8 (5)*
C(1c)	0.5060 (7)	0.7143 (9)	0.0658 (6)	4.1 (4)*	C(21e)	0.4856 (7)	0.488 (1)	0.2256 (6)	4.9 (4)*
C(2c)	0.4616 (7)	0.6983 (9)	0.0255 (6)	4.0 (4)*	Mn(1f)	0.4314 (1)	0.9286 (1)	0.27868 (9)	4.50 (9)
C(3c)	0.4719 (7)	0.687 (1)	−0.0140 (6)	5.0 (4)*	Mn(2f)	0.3642 (1)	0.7698 (2)	0.2342 (1)	5.55 (9)
C(4c)	0.5211 (8)	0.688 (1)	−0.0176 (6)	5.7 (5)*	O(1f)	0.4645 (4)	1.0369 (6)	0.2718 (3)	4.1 (4)
C(5c)	0.5656 (7)	0.702 (1)	0.0228 (6)	5.6 (4)*	O(2f)	0.3594 (4)	0.8571 (5)	0.2765 (3)	4.3 (4)
C(6c)	0.5593 (7)	0.7188 (9)	0.0652 (6)	4.5 (4)*	O(3f)	0.3781 (4)	0.6509 (6)	0.2170 (4)	4.9 (4)
C(7c)	0.6461 (7)	0.7710 (9)	0.1073 (6)	4.2 (6)	N(1f)	0.3729 (5)	1.0173 (7)	0.2849 (4)	3.9 (4)
C(8c)	0.6921 (7)	0.7985 (9)	0.1448 (6)	4.1 (4)*	N(2f)	0.3240 (5)	0.6976 (7)	0.2710 (5)	4.3 (5)
C(9c)	0.7338 (7)	0.8293 (9)	0.1341 (5)	4.1 (4)*	C(1f)	0.4327 (6)	1.0987 (9)	0.2605 (5)	3.7 (4)*
C(10c)	0.7806 (7)	0.8621 (9)	0.1673 (6)	4.3 (4)*	C(2f)	0.4449 (7)	1.1656 (9)	0.2457 (5)	4.6 (4)*
C(11c)	0.8262 (7)	0.898 (1)	0.1557 (6)	5.9 (6)	C(3f)	0.4073 (8)	1.226 (1)	0.2348 (6)	6.2 (5)*
C(12c)	0.7824 (6)	0.8622 (9)	0.2130 (5)	4.1 (4)*	C(4f)	0.3591 (7)	1.221 (1)	0.2402 (6)	5.8 (5)*

Table II (Continued)

atom	x/a	y/b	z/c	B, Å²	atom	x/a	y/b	z/c	B, Å²
C(5f)	0.3478 (7)	1.153 (1)	0.2581 (6)	5.5 (4)*	O(1ac)	0.6166 (8)	0.702 (1)	0.2728 (6)	11.2 (8)
C(6f)	0.3837 (6)	1.0883 (9)	0.2683 (5)	3.9 (4)*	O(2ac)	0.5404 (7)	0.6859 (8)	0.2704 (5)	8.8 (6)
C(7f)	0.3416 (7)	1.010 (1)	0.3071 (6)	4.8 (6)	C(3ac)	0.410 (1)	0.924 (1)	0.1737 (8)	7 (1)
C(8f)	0.3266 (6)	0.9379 (9)	0.3221 (5)	3.4 (3)*	C(4ac)	0.372 (1)	0.979 (1)	0.1459 (8)	12 (1)
C(9f)	0.3023 (6)	0.9462 (9)	0.3551 (6)	4.6 (4)*	O(3ac)	0.4510 (5)	0.8994 (7)	0.1662 (4)	6.6 (5)
C(10f)	0.2798 (7)	0.882 (1)	0.3706 (6)	5.3 (4)*	O(4ac)	0.4031 (5)	0.8926 (7)	0.2078 (4)	6.9 (4)
C(11f)	0.2518 (9)	0.896 (1)	0.4041 (6)	8.1 (9)	O(w)	0.503 (1)	0.197 (2)	0.771 (1)	27 (1)*
C(12f)	0.2831 (6)	0.8126 (9)	0.3490 (6)	4.8 (4)*	O(et1)	0.830 (1)	0.267 (2)	0.584 (1)	18.8 (9)*
C(13f)	0.3082 (7)	0.801 (1)	0.3190 (6)	4.4 (4)*	C(1et1)	0.821 (2)	0.334 (3)	0.610 (2)	18 (2)*
C(14f)	0.3330 (6)	0.8651 (9)	0.3044 (5)	3.5 (4)*	C(1'et1)	0.791 (6)	0.354 (9)	0.554 (5)	10 (4)*
C(15f)	0.3071 (7)	0.722 (1)	0.3024 (6)	4.5 (6)	C(2et1)	0.770 (2)	0.377 (3)	0.580 (2)	16 (2)*
C(16f)	0.3203 (7)	0.620 (1)	0.2572 (6)	4.6 (4)*	C(2'et1)	0.736 (7)	0.43 (1)	0.518 (6)	13 (6)*
C(17f)	0.2917 (8)	0.561 (1)	0.2713 (6)	6.7 (5)*	C(3et1)	0.884 (2)	0.224 (3)	0.614 (2)	21 (2)*
C(18f)	0.2917 (8)	0.484 (1)	0.2549 (6)	6.6 (5)*	C(4et1)	0.881 (2)	0.164 (3)	0.584 (2)	24 (2)*
C(19f)	0.3190 (8)	0.468 (1)	0.2293 (6)	6.3 (5)*	O(et2)	0.027 (1)	0.163 (2)	0.917 (1)	24 (1)*
C(20f)	0.3449 (7)	0.520 (1)	0.2102 (6)	6.5 (5)*	C(1et2)	0.065 (2)	0.054 (3)	0.948 (2)	23 (2)*
C(21f)	0.3465 (7)	0.602 (1)	0.2291 (6)	4.9 (4)*	C(2et2)	0.030 (2)	0.105 (3)	0.955 (2)	23 (2)*
C(1ac)	0.586 (1)	0.664 (1)	0.2869 (8)	6.6 (9)	C(3et2)	0.000 (2)	0.241 (3)	0.919 (2)	18 (2)*
C(2ac)	0.601 (2)	0.603 (2)	0.315 (1)	15 (2)	C(4et2)	−0.005 (1)	0.277 (2)	0.871 (1)	16 (1)*

[a] Starred values indicate atoms were refined isotropically. Anisotropically refined atoms are given in the form of the isotropic equivalent displacement parameter defined as $B = 8\pi^2(U_{11}U_{22}U_{33})^{1/3}$; U_{11}, U_{22}, and U_{33} are mean-square displacements. The prime refers to the second position of the disordered atoms of the ethyl ether molecules.

As evidenced by Figure 3, both manganese coordination polyhedra of each binuclear unit include approximately square-planar NO_3 bases involving one nitrogen atom (N(1) or N(2)), two oxygen atoms (O(2) and O(1) or O(3)) originating from the L ligand, and a third oxygen atom O(4) originating from a hydroxo group (binuclear units A, C, D, and E) or O(Ac) originating from an acetate anion (binuclear units B and F). The O(2)–O(4) (or O(2)–O(ac)) edge is shared by the two aformentioned NO_3 basis planes of each binuclear unit. The coordination sphere of both manganese atoms of each binuclear unit is completed with oxygen atoms pertaining to one or two of the other five binuclear units.

The eighteen oxygen atoms of the six L ligands are divided into three groups: (i) the six O(2) atoms bridging two manganese(II) ions of the same binuclear unit are μ_2; (ii) the O(1a), O(1b), O(1d), O(1f) and O(3a), O(3c), O(3d), O(3e) atoms bridging two manganese(II) ions from different binuclear units are also μ_2; (iii) the O(1c), O(1e) and O(3b), O(3f) atoms bridging three manganese(II) ions pertaining to three different binuclear units are μ_3.

The four hydroxo oxygen atoms, O(4a), O(4c), O(4d), O(4e), bridging two manganese(II) ions of the same binuclear unit with a third manganese(II) ion pertaining to another binuclear unit are μ_3.

The two acetate anions are inequivalent: O(3Ac) and O(4Ac) are bonded to both manganese ions of units B and F, respectively. Thus, they are μ_2 and the corresponding acetate anion is bis-bidentate. On the other hand, O(1Ac) and O(2Ac) are bonded to one manganese (Mn(2c) and Mn(2e), respectively) with a syn-anti conformation, the corresponding acetate anion being bidentate.

The range of manganese–oxygen distances (2.02–2.90 Å, Table III) is larger than that usually observed for manganese(II) (2.00–2.50 Å).[8] However, as expected, the largest Mn–O distances are those involving manganese and oxygen atoms pertaining to different binuclear units.

The space arrangement of the six binuclear units constituting the dodecanuclear aggregate corresponds to a 10 Å radius sphere where the hydrocarbon ring moieties of the L ligands are peripheral (Figure 2a) and surround the manganese–oxygen–nitrogen core shown in Figure 2b. The twelve manganese(II) ions are arranged into two crowns of six metal ions, these two crowns being held together by ten oxygen atoms (O(3b), O(3f), O(1c), O(1e), O(4a), O(4c), O(4d), O(4e), O(2a), and O(2d)). The six oxygen atoms (O(1a), O(1b), O(1d), O(1f), O(2b), and O(2f)) are peripheral to the crown capped by the bis-bidentate acetate anion, while the six remaining oxygen atoms (O(3a), O(3c), O(3d), O(3e), O(2c), and O(2e)) are peripheral to the crown capped by the bidentate bridging acetate anion. Consequently, each of the twelve manganese(II) ions is oxygen-bridged to four nearest manganese(II) neighbors with manganese–manganese distances ranging from 3.16 to 4.14 Å (Table IV).

The stability of the dodecanuclear aggregate results presumably from (i) the flexibility of the L ligand, (ii) the large number of Mn–O bonds (58) and their extented range, (iii) the trend of manganese(II) toward hexacoordination.

On the grounds of their similarities, the six binuclear units constituting the dodecanuclear aggregate can be divided into three sets characterized by different geometries and/or nature of the coordination sphere of the manganese ions: (A, D), (B, F), and (C, E), as evidenced by Figure 3.

Binuclear Units A and D (Figure 3a,d). The manganese(II) ions are in a distorted octahedral NO_5 ligand environment characterized by two inequivalent axial Mn–O bonds. The short axial Mn–O bond is in the range 2.07–2.11 Å, while the long one is in the range 2.49–2.90 Å (Table III). The two manganese(II) ions of each A and D binuclear unit are located out of the NO_3 ligand plane in opposite directions with Mn–ligand plane distances ranging from 0.163 to 0.505 Å.[20]

In both A and D units, the L ligand is not planar, the dihedral angle between the phenyl ring planes ranging from 153 to 175°.[20] The intrabinuclear Mn–Mn distance is equal to 3.176 (4) Å for units A and D (Table IV).

Binuclear Units B and F (Figure 3b,f). The two manganese(II) ions of B and F binuclear units experience NO_5 ligand environments with different geometries. While the coordination polyhedron of Mn(1b) and Mn(1f) can be better viewed as a trigonal prism than as a distorted octahedron, the Mn(2b) and Mn(2f) coordination polyhedra can be better described as rhombically distorted octahedra. The distortion of the L ligand from a plane is the largest in units B and F, with dihedral angles between the phenyl ring planes ranging from 133.1 to 176°.[20] The manganese to NO_3 ligand plane distances (0.102 (3)–0.880 (3) Å) are also very large in units B and F.[20] The intrabinuclear Mn–Mn distances for units B (3.248 (3) Å) and F (3.279 (3) Å) are the largest intrabinuclear Mn–Mn distances in the dodecanuclear aggregate (Table IV).

The binuclear units B and F are bridged by a bis-bidentate acetate anion, each acetate oxygen being bonded to both manganese ions of binuclear units B and F.

Binuclear Units C and E (Figure 3c,e). The manganese(II) ions Mn(1c) and Mn(1e) are in a distorted NO_4 pyramidal environment including the NO_3 basis ligand plane and an axial oxygen atom from the L ligand of units A and D. Mn(1c) and Mn(1e) are 0.691 (3) and 0.550 (3) Å out of the NO_3 ligand plane, respectively.[20] The manganese(II) ions Mn(2c) and Mn(2e) are in an NO_5 octahedral ligand environment. One axial oxygen is afforded by the bidentate acetate, thus bridging units C and E

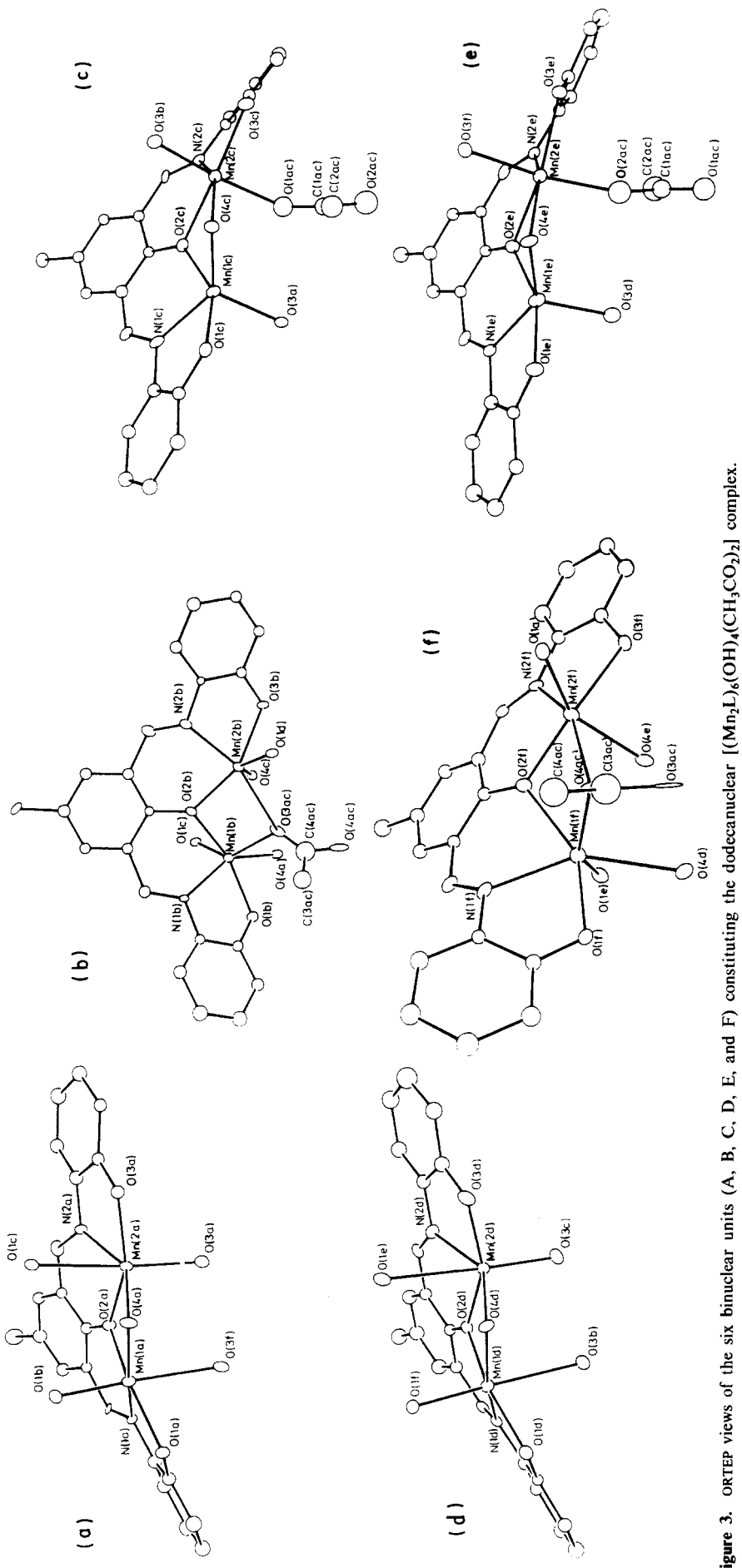

Figure 3. ORTEP views of the six binuclear units (A, B, C, D, E, and F) constituting the dodecanuclear $[(Mn_2L)_6(OH)_4(CH_3CO_2)_2]$ complex.

Table III. Selected Bond Distances (Å) (Manganese Environment)

Mn(1a)–N(1a)	2.18 (1)	Mn(1a)–O(1a)	2.16 (1)	Mn(1d)–O(1d)	2.12 (2)	Mn(1d)–O(2d)	2.142 (9)
Mn(1a)–O(2a)	2.14 (1)	Mn(1a)–O(4a)	2.11 (1)	Mn(1d)–O(4d)	2.12 (1)	Mn(1d)–O(1f)	2.14 (1)
Mn(1a)–O(3f)	2.49 (1)	Mn(1a)–O(1b)	2.11 (1)	Mn(1d)–O(3b)	2.58 (1)	Mn(2d)–N(2d)	2.19 (1)
Mn(2a)–N(2a)	2.19 (2)	Mn(2a)–O(2a)	2.173 (9)	Mn(2d)–O(2d)	2.12 (1)	Mn(2d)–O(3d)	2.10 (1)
Mn(2a)–O(3a)	2.13 (2)	Mn(2a)–O(4a)	2.11 (2)	Mn(2d)–O(4d)	2.085 (8)	Mn(2d)–O(1e)	2.90 (1)
Mn(2a)–O(1c)	2.76 (1)	Mn(2a)–O(3e)	2.08 (1)	Mn(2d)–O(3c)	2.07 (1)	Mn(1e)–N(1e)	2.14 (2)
Mn(1b)–N(1b)	2.23 (1)	Mn(1b)–O(1b)	2.11 (2)	Mn(1e)–O(1e)	2.10 (2)	Mn(1e)–O(2e)	2.06 (2)
Mn(1b)–O(2b)	2.27 (1)	Mn(1b)–O(3ac)	2.14 (1)	Mn(1e)–O(4e)	2.02 (2)	Mn(1e)–O(3d)	2.07 (1)
Mn(1b)–O(4a)	2.42 (1)	Mn(1b)–O(1c)	2.11 (2)	Mn(2e)–N(2e)	2.22 (1)	Mn(2e)–O(2e)	2.29 (1)
Mn(2b)–N(2b)	2.19 (2)	Mn(2b)–O(2b)	2.08 (2)	Mn(2e)–O(3e)	2.19 (1)	Mn(2e)–O(4e)	2.30 (1)
Mn(2b)–O(3b)	2.228 (8)	Mn(2b)–O(3ac)	2.43 (1)	Mn(2e)–O(2ac)	2.21 (2)	Mn(2e)–O(3f)	2.206 (9)
Mn(2b)–O(1d)	2.12 (2)	Mn(2b)–O(4c)	2.14 (2)	Mn(1f)–N(1f)	2.24 (1)	Mn(1f)–O(1f)	2.11 (2)
Mn(1c)–N(1c)	2.16 (2)	Mn(1c)–O(1c)	2.220 (8)	Mn(1f)–O(2f)	2.26 (1)	Mn(1f)–O(4ac)	2.15 (1)
Mn(1c)–O(2c)	2.12 (1)	Mn(1c)–O(4c)	2.06 (1)	Mn(1f)–O(1e)	2.09 (1)	Mn(1f)–O(4d)	2.49 (1)
Mn(1c)–O(3a)	2.06 (2)	Mn(2c)–N(2c)	2.20 (1)	Mn(2f)–N(2f)	2.22 (2)	Mn(2f)–O(2f)	2.04 (2)
Mn(2c)–O(2c)	2.24 (1)	Mn(2c)–O(3c)	2.17 (1)	Mn(2f)–O(3f)	2.19 (2)	Mn(2f)–O(4ac)	2.62 (1)
Mn(2c)–O(4c)	2.292 (9)	Mn(2c)–O(3b)	2.15 (2)	Mn(2f)–O(4e)	2.11 (2)	Mn(2f)–O(1a)	2.077 (9)
Mn(2c)–O(1ac)	2.11 (2)	Mn(1d)–N(1d)	2.16 (1)				

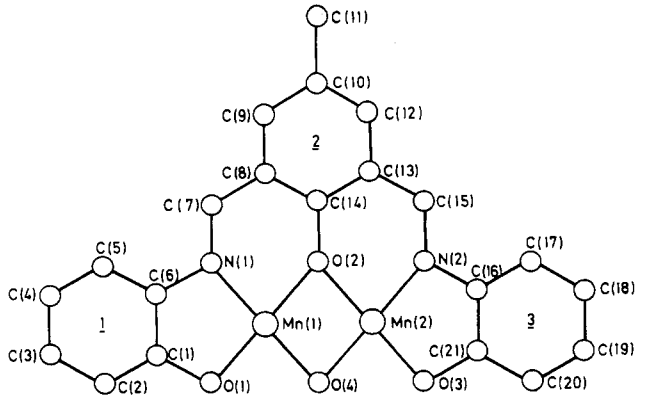

Figure 4. Full labeling scheme for the binuclear units.

Table IV. Distances (Å) between Oxygen-Bridged Manganese Atoms

Mn(1a)–Mn(2a)	3.176 (4)	Mn(1a)–Mn(1b)	3.383 (4)
Mn(1a)–Mn(2e)	4.046 (3)	Mn(1a)–Mn(2f)	3.164 (4)
Mn(2a)–Mn(1b)	3.688 (4)	Mn(2a)–Mn(1c)	3.347 (4)
Mn(2a)–Mn(2e)	3.586 (4)	Mn(1b)–Mn(2b)	3.248 (3)
Mn(1b)–Mn(1c)	3.517 (3)	Mn(2b)–Mn(1c)	3.654 (4)
Mn(2b)–Mn(2c)	3.387 (3)	Mn(2b)–Mn(1d)	3.179 (4)
Mn(1c)–Mn(2c)	3.201 (3)	Mn(2c)–Mn(1d)	4.143 (4)
Mn(2c)–Mn(2d)	3.536 (4)	Mn(1d)–Mn(2d)	3.176 (3)
Mn(1d)–Mn(1f)	3.369 (4)	Mn(2d)–Mn(1e)	3.338 (5)
Mn(2d)–Mn(1f)	3.848 (3)	Mn(1e)–Mn(2e)	3.195 (4)
Mn(1e)–Mn(1f)	3.326 (3)	Mn(1e)–Mn(2f)	3.503 (3)
Mn(2e)–Mn(2f)	3.381 (4)	Mn(1f)–Mn(2f)	3.279 (3)

Table V. Manganese–Oxygen–Manganese Bridging Angles (deg)

Mn(1a)–O(2a)–Mn(2a)	95.0 (4)	Mn(1a)–O(4a)–Mn(2a)	97.7 (4)
Mn(1a)–O(4a)–Mn(1b)	96.6 (4)	Mn(1a)–O(3f)–Mn(2e)	118.8 (5)
Mn(1a)–O(3f)–Mn(2f)	84.8 (3)	Mn(2a)–O(4a)–Mn(1b)	109.3 (5)
Mn(2a)–O(3a)–Mn(1c)	106.4 (4)	Mn(2a)–O(3e)–Mn(2e)	114.6 (4)
Mn(1b)–O(2b)–Mn(2b)	96.6 (5)	Mn(1b)–O(3ac)–Mn(2b)	90.6 (5)
Mn(2b)–O(4c)–Mn(1c)	120.7 (6)	Mn(2b)–O(3b)–Mn(2c)	101.5 (4)
Mn(2b)–O(4c)–Mn(2c)	99.6 (5)	Mn(2b)–O(1d)–Mn(1d)	97.5 (4)
Mn(2b)–O(3b)–Mn(1d)	82.5 (3)	Mn(1c)–O(2c)–Mn(2c)	94.3 (5)
Mn(1c)–O(4c)–Mn(2c)	94.5 (4)	Mn(2c)–O(3b)–Mn(1d)	122.3 (6)
Mn(2c)–O(3c)–Mn(2d)	112.9 (4)	Mn(1d)–O(2d)–Mn(2d)	96.4 (4)
Mn(1d)–O(4d)–Mn(2d)	98.2 (4)	Mn(1d)–O(4d)–Mn(1f)	93.8 (4)
Mn(2d)–O(1e)–Mn(1e)	82.1 (4)	Mn(2d)–O(3d)–Mn(1e)	106.4 (4)
Mn(2d)–O(1e)–Mn(1f)	99.7 (5)	Mn(2d)–O(4d)–Mn(1f)	114.4 (6)
Mn(1e)–O(2e)–Mn(2e)	94.8 (5)	Mn(1e)–O(4e)–Mn(2e)	95.4 (4)
Mn(1e)–O(1e)–Mn(1f)	104.9 (4)	Mn(1e)–O(4e)–Mn(1f)	82.8 (3)
Mn(1e)–O(4e)–Mn(2f)	116.3 (6)	Mn(2e)–O(4e)–Mn(1f)	178.1 (5)
Mn(2e)–O(3f)–Mn(2f)	100.7 (4)	Mn(2e)–O(4e)–Mn(2f)	100.3 (4)
Mn(1f)–O(2f)–Mn(2f)	99.4 (5)	Mn(1f)–O(4ac)–Mn(2f)	86.2 (4)
Mn(1f)–O(4e)–Mn(2f)	79.9 (3)		

through Mn(2c) and Mn(2e), while the second axial oxygen pertains to the L ligand of units F or B.

The intrabinuclear Mn–Mn distances, 3.201 (3) and 3.195 (4) Å, respectively (Table IV), are very similar in units C and E and intermediate between the distances observed for the units A and D, on the one hand, and B and F, on the other hand.

Magnetic Susceptibility Measurements. The effective magnetic moment per manganese(II) ion (5.62 μ_B/Mn[20]) is lower than the spin-only value at room temperature. The decrease in effective magnetic moment with decreasing temperature is regular over the whole temperature range and results in a 1.39 μ_B/Mn effective magnetic moment at 5 K, indicating that the net antiferromagnetic exchange interaction is quite large.

As already mentioned in the molecular structure section, each of the twelve manganese(II) ions present in this aggregate is oxygen-bridged to four nearest manganese neighbors. All twenty-four ions present in this aggregate are oxygen-bridged to four nearest manganese neighbors. All twenty-four distances between oxygen-bridged manganese(II) ions are different and range between 3.164 (4) and 4.143 (4) Å (Table IV). The corresponding MnOMn angles are in the range 82.1–178.1° (Table V). The dihedral angles between the planes defined by one manganese ion and the bridging oxygen atoms, on the one hand, and the second

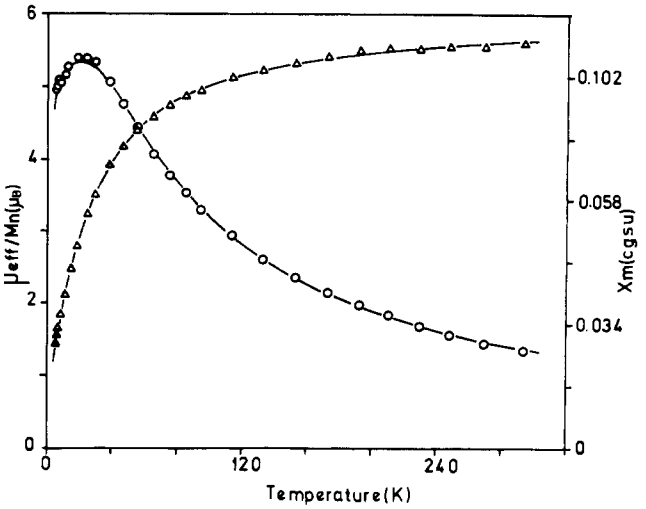

Figure 5. Variable-temperature magnetic susceptibility data for $[(Mn_2L)_6(OH)_4(CH_3CO_2)_2]$. The solid lines result from a least-squares fit of the data to the theoretical equation for isotropic magnetic exchange in a binuclear complex with $S_1 = S_2 = {}^5/_2$.

manganese ion and the same bridging oxygen atoms, on the other hand, are in the range 119.7–169.8°.[20] Consequently, twenty-four different Mn(II)–Mn(II) magnetic interactions can be transmitted through the bridging oxygen ligands.

The bulk magnetic susceptibility measurements afford the average value of the magnetic interactions present in this aggregate. The large decrease in effective magnetic moment with decreasing temperature indicates that, among the twenty-four possible magnetic interactions, the antiferromagnetic interactions are largely prevailing against the ferromagnetic ones.

Consequently, the interpretation of the variation of the magnetic susceptibility with temperature was attempted by using the magnetic susceptibility equation for a Heisenberg-type chain.[21] The least-squares fitting of the experimental data to the equation for a chain did not afford any reasonable results, indicating that an infinite chain approximation is not valid in the case of this spherical aggregate. Finally, the experimental magnetic susceptibility data were least-squares-fit to the theoretical equation for an isotropic magnetic exchange interaction between two $S_1 = S_2 = {}^5/_2$ ions by employing the $\mathcal{H} = -2JS_1S_2$ spin Hamiltonian.[22] The aim of this oversimplified approach was to get an average value of the magnetic interactions operating in this aggregate. The lines in Figure 5 represent this fit, which can be seen to be good. The parameters obtained from the fit are $J = -3.0$ cm^{-1} and $g = 1.91$; the 1.91 g value is low compared to the 2.01 value measured from the X-band powder EPR spectra. However, this oversimplified approach affords an estimate of the average value of the magnetic interactions operating in this aggregate.

EPR Spectroscopy. The X-band and Q-band powder EPR spectra (300 and 120 K) exhibit a narrow isotropic resonance centered at $g = 2.01$ (Figure 6a), the total width of the resonance being 300 G at X-band. The DMF–toluene glass spectra also are characterized by a unique and narrow isotropic resonance devoid of any hyperfine structure independently of the concentration of the solutions (Figure 6b). This unusual EPR behavior has already been reported for systems consisting of N divalent manganese(II) ions coupled together by exchange interactions[23–27] and has been rationalized for the first time by Kubo and Tomita,[28] who have set up the basis of the theory used to explain the exchange-nar-

(21) Wagner, G. R.; Friedberg, S. A. *Phys. Lett.* **1964**, *9*, 11–13.
(22) Spiro, C. L.; Lambert, S. L.; Smith, T. J.; Duesler, E. N.; Gagné, R. R.; Hendrickson, D. N. *Inorg. Chem.* **1981**, *20*, 1229–1237.
(23) Gorter, C. J.; Van Vleck, J. H. *Phys. Rev.* **1947**, *72*, 1128–1129.
(24) Van Vleck, J. H. *Phys. Rev.* **1948**, *74*, 1168–1183.
(25) Van Wieringen, J. S. *Discuss. Faraday Soc.* **1955**, *19*, 118–126.
(26) Matumura, O. *Mem. Fac. Sci. Kyushu Univ.* **1958**, *B2*, 175–179.
(27) Schneider, E. E.; England, T. S. *Physica* **1951**, *17*, 221–233.
(28) Kubo, R.; Tomita, K. *J. Phys. Soc. Jpn.* **1954**, *9*, 888–919.

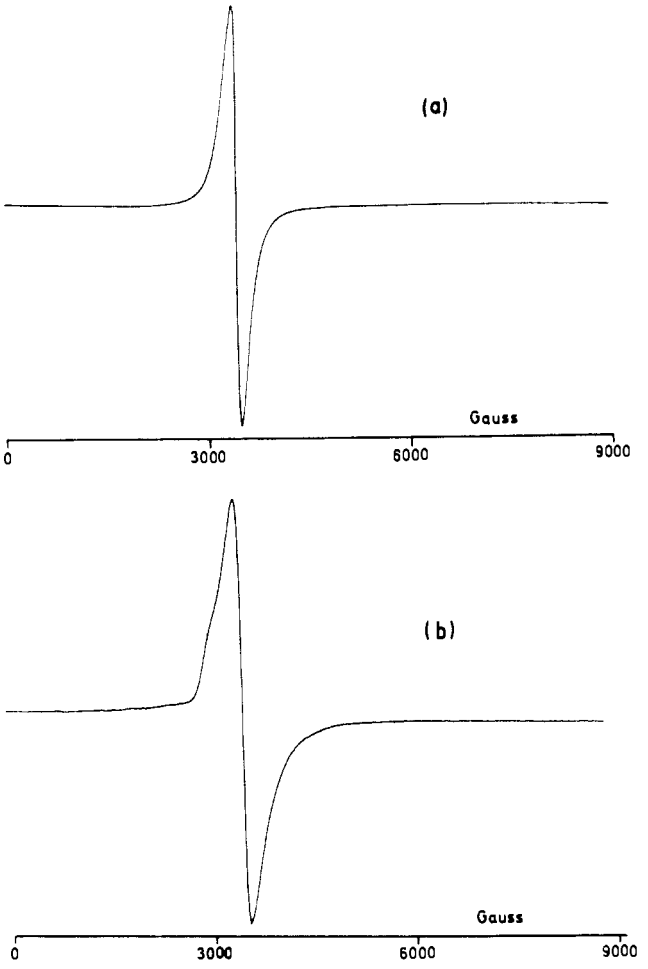

Figure 6. X-Band EPR spectra of $[(Mn_2L)_6(OH)_4(CH_3CO_2)_2]$: (a) powder at 110 K (microwave power 1 mW, microwave frequency 9.426 GHz, 10-G modulation amplitude); (b) DMF/toluene glass at 110 K (microwave power 2.5 mW, microwave frequency 9.424 GHz, 4-G modulation amplitude).

rowing phenomenon.[29] However, Ishikawa[30] has shown that when the anisotropic interactions are negligible and the exchange integrals are much larger than the hyperfine constant ($|J_{ij}| \gg |A|$), which is presently the case, the system may be regarded as being approximately in an eigenstate of S^2 and S_z. According to this approximation, the hyperfine term in the approximate spin Hamiltonian should be A/NS_zI_z rather than $A\sum S_{iz}I_{iz}$ where I ($=^5/_2$) is the nuclear spin quantum number of an isolated manganese ion. At fixed microwave frequency (ν) and variable magnetic field (H), the resonance absorption lines are at $H = H_0 - (A'/N)m$ where $H_0 = h\nu/g\beta$, $A' = A/g\beta$, and $m = A\sum m_i$ where m_i is the nuclear magnetic quantum number of the individual ion. Thus there are $2NI + 1$ hyperfine structure lines with equal separation of A/N. The relative intensities of the hyperfine lines corresponding to each m are given by the number of ways of building up each m. The expected hyperfine structure will not be distinguishable unless there is exchange narrowing of each individual hyperfine line.

(29) Pake, G. E. In *Paramagnetic Resonance*; Pines, D., Ed.; Benjamin: Reading, MA, 1962; pp 89–95, 140–152.
(30) Ishikawa, Y. *J. Phys. Soc. Jpn.* **1966**, *21*, 1473–1481.

Concluding Remarks

Each manganese(II) ion of the dodecanuclear aggregate described in this paper is oxygen-bridged to four nearest manganese neighbors. This leads to twenty-four Mn···Mn distances ranging from 3.16 to 4.14 Å. As evidenced by the magnetic susceptibility study, this structural arrangement affords a large predominance of the antiferromagnetic interactions in the aggregate. EPR spectroscopy evidences for the first time the exchange narrowing of frozen-solution polynuclear manganese spectra. To our knowledge, this is the first frozen-solution example of the inhomogeneous exchange-narrowing situation described by Ishikawa.[30]

Finally, it is of interest to note that this complex is the first polynuclear manganese compound built from an acyclic polydentate ligand. All previous examples of polynuclear manganese complexes are based on either macrocyclic ligands,[7,31] combinations of carboxylates and oxides involving or not involving additional terminal monodentate or bidentate ligands,[32–36] fluoride and terminal monodentate ligands,[37] fluoride and hydroxide and terminal carbonyl ligands,[38] or thiolate ligands.[39]

Acknowledgment. We thank the Etablissement Public Régional and the Action de Recherche Intégrée "Chimie-Biologie" for partial support of this work. J. Aussoleil and F. Dahan are gratefully acknowledged for the writing of several structure subroutines. Ph. de Loth is to be thanked for the writing of magnetic susceptibility subroutines.

Supplementary Material Available: Figure 7, showing an ORTEP view of the unit cell of $[(Mn_2L)_6(OH)_4(CH_3CO_2)_2]$, Table VI, listing the experimental magnetic susceptibility data, Tables VII–XI, listing crystallographic data, thermal parameters, hydrogen positions, interatomic distances and angles, and main planes in and between binuclear units (59 pages); Table XII, listing observed and calculated structure factors (35 pages). Ordering information is given on any current masthead page.

(31) (a) McKee, V.; Shepard, W. B. *J. Chem. Soc., Chem. Commun.* **1985**, 158–159. (b) Brooker, S.; McKee, V.; Shepard, W. B.; Pannell, L. K. *J. Chem. Soc., Dalton Trans.* **1987**, 2555–2562.
(32) (a) Lis, T.; Jezowska-Trzebiatowska, B. *Acta Crystallogr., Sect. B* **1977**, *33*, 2112–2116. (b) Lis, T. *Acta Crystallogr., Sect. B* **1980**, *36*, 2042–2046.
(33) (a) Baikie, A. R. E.; Hursthouse, M. B.; New, D. B.; Thornton, P. *J. Chem. Soc., Chem. Commun.* **1978**, 62. (b) Baikie, A. R. E.; Hursthouse, M. B.; New, L.; Thornton, P.; White, R. G. *J. Chem. Soc., Chem. Commun.* **1980**, 684–685. (c) Vincent, J. B.; Chang, H. R.; Folting, K.; Huffman, J. C.; Christou, G.; Hendrickson, D. N. *J. Am. Chem. Soc.* **1987**, *109*, 5703–5711.
(34) Baikie, A. R. E.; Howes, A. J.; Hursthouse, M. B.; Quick, A. B.; Thornton, P. *J. Chem. Soc., Chem. Commun.* **1986**, 1587.
(35) Christmas, C.; Vincent, J. B.; Huffman, J. C.; Christou, G.; Chang, H. R.; Hendrickson, D. N. *Angew. Chem., Int. Ed. Engl.* **1987**, *26*, 915–916.
(36) Vincent, J. B.; Christmas, C.; Huffman, J. C.; Christou, G.; Chang, H. R.; Hendrickson, D. N. *J. Chem. Soc., Chem. Commun.* **1987**, 236–238. (b) Christmas, C.; Vincent, J. B.; Huffman, J. C.; Christou, G.; Chang, H. R.; Hendrickson, D. N. *J. Chem. Soc., Chem. Commun.* **1987**, 1303–1305. (c) Bashkin, J. S.; Chang, H. R.; Streib, W. E.; Huffman, J. C.; Hendrickson, D. N.; Christou, G. *J. Am. Chem. Soc.* **1987**, *109*, 6502–6504.
(37) (a) Smit, J. J.; Nap, G. M.; De Jongh, L. J.; Van Ooijen, J. A. C.; Reedijk, J. *Physica* **1979**, *97B*, 365–376. (b) Ten Hoedt, R. W. M.; Reedijk, J. *Inorg. Chim. Acta* **1981**, *51*, 23–27.
(38) Horn, E.; Snow, M. R.; Zeleny, P. C. *Aust. J. Chem.* **1980**, *33*, 1659–1665.
(39) Costa, T.; Dorfman, J. R.; Hagen, K. S.; Holm, R. H. *Inorg. Chem.* **1983**, *22*, 4091–4099.